

Lessons on internal erosion in embankment dams from failures and physical models

J.J. Fry

EDF-CIH 73 373 Cedex, Le Bourget du Lac, France

ABSTRACT: The investigations of embankment failures reported by Erinoh R&D project, merged with the Foster & Fell Erdata and NPDP program in the USA, point out the main causes and the main situations where internal erosion could initiate and trigger the failure of dams. The investigation of physical models built in the CACOH laboratory of CNR shows under particular circumstances (piping at core base) pervious shells cannot provide enough weight or erosion resistance to resist concentrated leaks. Three different mechanisms of failure may occur: (1) general instability without hydraulic fracturing, (2) hydraulic fracturing (with or without suffusion) followed by piping, (3) backward erosion or sloughing (surface instability). Physical models help to understand the conditions and the physical situations in which each of these three modes of failure apply. This paper relates to these physical tests and presents the main results and conclusions.

1 INTRODUCTION

Internal erosion is a major cause of failures of water retaining structures. Around half of the failures are caused by internal erosion (piping) and half are caused by external erosion (overtopping); failures by sliding are infrequent.

According to the International Commission on Large Dams (ICOLD 1995), an 'incident' is either a 'failure' or an 'accident' requiring repair. A 'failure' is a collapse or movement of part of a dam or its foundation, to the extent that the dam cannot retain water. An 'accident' occurs, when a failure is prevented by immediate remedial measures, possibly including drawing down the water. A large dam is a dam which is more than 15 meters in height (measured from the lowest point in the general foundations to the crest of the dam).

Many failures of embankment dams were triggered by internal erosion. For instance in France, at the end of the last century, there was around one breach of a water retaining structure (flood embankments, navigation canal embankments or small dams) per year caused by internal erosion. Moreover, internal erosion is a threat not clearly defined and understood. For instance, analysis of stability is well-known and has been studied and taught at universities for a long time; in contrast, analysis of internal erosion was reduced to the study of uplift by Terzaghi and the piping rules of Lane and Bligh. To fill that gap, the Erinoh project was launched.

That national research project was launched in 2006 and completed in 2012 in order to better understand the mechanisms of internal erosion and to reduce the damages caused by that hazard. Erinoh was responsible for bringing together partners, such as universities, owners and engineering offices, to investigate the mechanisms of internal erosion in dams, dikes and their foundations and to propose engineering solutions to reduce the impact of that hazard.

Erinoh's first task was to assemble, a database of internal erosion incidents, accidents and failures caused by internal erosion and by external erosion (overtopping) of water retaining structures, such as dams or dikes of retaining navigation or hydroelectric canals and flood embankments or levees, mainly in France.

In this paper, case studies are taken and statistics are calculated from the compilation of ICOLD Technical Bulletin 99 (ICOLD, 1995), Technical Bulletin 164 (ICOLD, 2015), the Erdata base (Foster et al, 1998), the NPDP program in the USA (Richards & Reddy, 2007) and the Erinoh database on incidents developed by Paul Royet and the author.

Internal erosion is commonly thought to be a hazard that could strike an embankment dam at any time. However, careful investigation shows that internal erosion occurred mostly in particular situations (geology, design and loadings). The purpose of the first part of this paper is to point out the principal situations where failures by internal erosion were observed.

Mechanisms of internal erosion are hidden. Thus the main difficulty is to understand the different phases of development. To overcome that difficulty, physical models were built and tested in a laboratory with a 1/1 to 1/10 scale in order to understand the whole process.

The purpose of the second part of this report is to point out the principal observations and conclusions on contact erosion and suffusion mechanisms.

2 LESSONS FROM DAM FAILURES

2.1 Omission of filters is the primary cause of internal erosion failures

First of all, it is very important to underline that all the case histories reported in the Erinoh data base of failures of water retaining structures caused by internal erosion, showed no evidence of filters in the failed embankments, this is true of both for dams and dikes. For instance, all the failures of Loire levees (1846, 1856, 1866) involve heterogeneous embankments, built and raised over the centuries, without any filters and all the failures along the Rhone river (1993,1994, 2002, 2004) occurred in flood embankment without any filters.

At first glance, this is not the case, for all the internal erosion failures of large dams, as reported by Foster et al. (1998). Five dams with filters failed: Baldwin Hills (1963), Teton (1976), Wadi Qattarah (1977) Quail Creek (1989), and Zoeknog (1993). These case studies are presented hereunder in order to understand why the filter was not effective in controlling internal erosion in those cases.

Baldwin Hills reservoir (H=47m at axis), watertight by a 3 m-thick compacted earth lining, was impounded in 1951. Several problems occurred from 1951 to 1963. The geological context, subject to tectonic and seismic activity, regional subsidence, nearby major active faults and underlain by low density, dispersive residuals soils, is extremely difficult. An estimated maximum settlement of about 90 cm at the reservoir occurred between 1917 and 1963, the S-W corner dropping more than the N-E corner. The reservoir stretched a max of about 25 cm in the S-W direction. The failure was the result of large movements on faults, possibly caused by oil extraction. The sand filter layer thickness was very small and completely inappropriate to control the very bad geology.

Teton dam is a zoned embankment (H=93m) impounded in 1976. The filter, omitted in the trench, was very thick under the shoulder. However, it was a natural alluvium with excessive % of plastic fines; its permeability was in some places as low as 10^{-7} m/s. It was placed on jointed rock, with open joints not always sealed with gunite or concrete. In consequence, the pipes, increasing from hydraulic fractures through the core, were stopped by the filter, the

flow was diverted into the unsealed cracks, passed the filter, exited on the downstream surface of the shell, developed backward erosion, and finally the hydraulic head below the filter fractured it.

Wadi Qattarah dam (H=38m) was a homogeneous dam impounded in 1977. The embankment was protected by a chimney filter, the foundation by a filter carpet. However, the conduit was put in a trench through the rocky foundation, below the filter carpet. The trench was filled with the slightly dispersive embankment fill material. The trench walls were fractured and not protected by gunite. Backward erosion initiated into the cracks, hydraulic cracking and concentrated leak (piping) occurred in the trench during the first impounding.

The Quail Creek zoned dam (H=25m) failed at the end of impounding after three grouting campaigns. The core containing up to 12% of salty soils (gypsum) was protected by a filter chimney but not by a filter carpet. As the excavated rocky foundation was very irregular, a series of troughs and peaks running from upstream to downstream, some layers of core material were placed between foundation and chimney filter to smooth the foundation surface. Those soil layers, no longer protected by filter, were eroded at contact of vertical fault gouges and gypsum layer in foundation.

Zoeknog dam case is similar to Wadi Qattarah. The outlet conduit was put in a trench through the foundation, below the filter carpet. The dispersive eolian silt was compacted around the outlet in the trench, whose the walls were not protected by gunite. Backward erosion initiated into the cracks, hydraulic cracking and concentrated leak occurred in the trench.

The assessment of the causes of failure of these five case studies show that in 3 cases, the filter was at the wrong location (3/5), in one case the geology was too bad for a dam site (1/5) and in the last case the transition was not pervious enough and was bypassed and fractured by high water head (1/5).

In conclusion, all the embankments designed without filter are at risk of failure by internal erosion. However, failure could occur where filter is at the wrong location. The filter is the most effective safety barrier against internal erosion, but it is not enough: other safety barriers are required to protect a dam against any failure mode, in such a matter safety is ensured by "belt and braces" (Table 1).

Table 1. The main safety barriers designed to avoid the 3 main modes of failure.

<i>Mode of failure</i>	<i>1st safety barrier</i>	<i>2nd safety barrier</i>
Sliding	Shoulder stability	Drainage
Internal erosion	Filter	Watertightness
External erosion	Spillway+freeboard	D/S protection

Watertightness is the second barrier. Without watertightness of the foundation and dam body, the filter could be by-passed in very pervious or cracked foundations and/or fractured by the reservoir head.

2.2 The most dangerous mechanism: the concentrated leak

Internal erosion initiates in four mechanisms: concentrated leak, backward erosion, contact erosion and suffusion (Fell & Fry 2007, ICOLD 2015, Fig. 1).

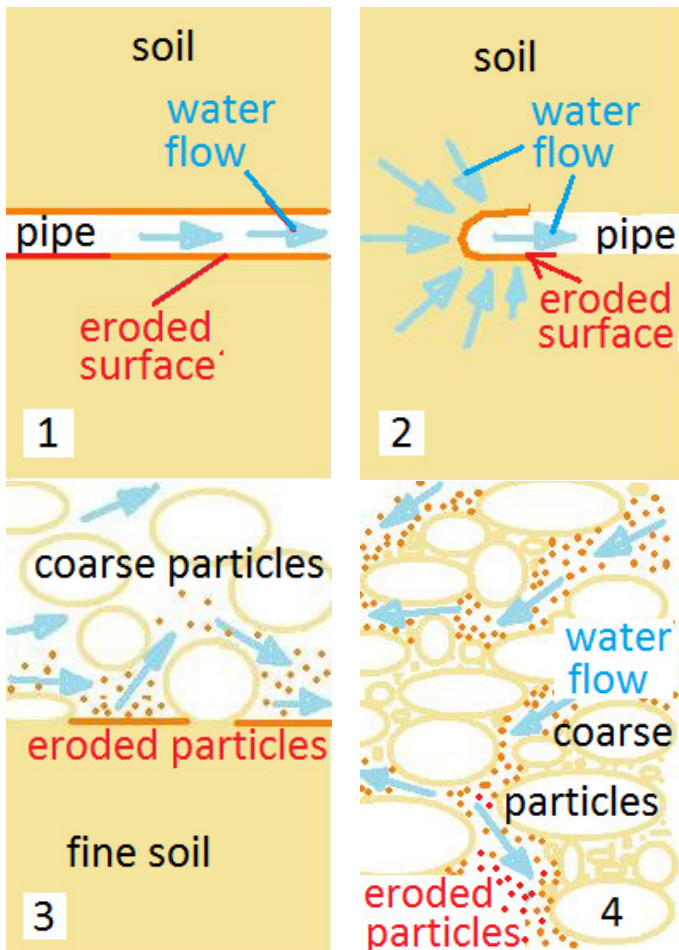


Figure 1. The Four mechanisms of internal erosion (Fell & Fry 2007).

1. Concentrated leak erosion, first initiating mechanism of erosion, occurs where the sides of an opening may be eroded by the concentrated leakage flow through the opening in saturated clayey soil, and sometimes in unsaturated silty soil.
2. Backward erosion involves the detachment of soils particles when the seepage exits to a free unfiltered surface, such as the ground surface of a sandy layer under a clayey dike, karsts in the foundation or the downstream face of a homogeneous embankment or a coarse rock fill zone.
3. Contact erosion (also known as parallel contact erosion) involves erosion of fine particles from

- the contact with a coarser layer, caused by the flow passing through the coarser layer.
4. Suffusion is erosion of internally unstable soils which involves selective erosion of finer particles from the matrix of coarser particles, in such a manner that the finer particles are removed through the voids between the larger particles by seepage flow, leaving behind a soil skeleton formed by the coarser particles.

The statistics of failures collected by Foster & al., the NPDP program and ERINOH database show clearly that the most dangerous mechanism is the concentrated leak (Table 2).

Table 2. Statistics of the initiating mechanisms of internal erosion causing failures

Mechanisms	All dams		Large dams		Small dams	
	N	%	N	%	N	%
Concentrated leak	169	46	35	31	139	54
Backward erosion	30	8	11	10	19	7
Contact erosion	29	8	14	13	11	4
Suffusion	4	1	1	1	5	2
Unknown	139	37	50	45	85	33
Total	371	100	111	100	259	100

Concentrated leaks occur in flaws and defects. What are the most drastic and dangerous flaws?

2.3 Openings along structures are the most dangerous flaws leading to failure

Statistics of failures collected by Foster & Fell, the NPDP program and the ERINOH database encompassed in Table 3 show that the number of defects in dam bodies leading to failure is 4-5 times larger than those in foundations.

Table 3. Statistics of the initiating path of internal erosion causing failures

Paths of internal erosion	All dams		Large		Small	
	N	%	N	%	N	%
Through the embankment	203	55	50	45	153	59
Through the foundation	44	12	18	16	26	10
embankment- foundation	5	1	5	5	0	0
Unknown	119	32	38	34	80	31
Total	371	100	111	100	259	100

The most dangerous defects are openings along structures (walls and aprons of spillways and conduits), followed by cracks through cohesive soils or geologically continuous voids in foundations (open faults, open vertical cracks, karsts). Erosion in openings alongside structures passing through embankments or foundations are the causes of one-third of the failures by internal erosion and one-half of the proven causes (Table 4).

Table 4. Locations of defects leading to failure (Foster et al., NPDP program and ERINOH database)

Locations	<i>All dams</i>		<i>Large dams</i>		<i>Small dams</i>	
	N	%	N	%	N	%
Conduit	87	24%	22	20%	65	25%
Core	8	2%	6	5%	2	1%
Spillway	29	8%	7	6%	22	8%
Fill	45	12%	6	5%	39	15%
Foundation	36	10%	14	13%	22	8%
Abutment	8	2%	6	5%	2	1%
Upstream slope	3	1%	3	3%	3	1%
Membrane	2	1%	2	2%	0	0
Crest	5	1%	5	5%	5	2%
Unknown	148	40%	40	36%	99	39%
Total	371	100%	111	100%	259	100%

Cracks and openings are triggered by two main phenomena:

- relative displacement and,
- hydraulic fracture.

2.4 Failures initiated in the dam body after 10 years of operation

Of the 35 failures of large dams, initiated by internal erosion in the embankment dam body within the 20th century, reported by Foster & Fell (1998), only 9 occurred after 10 years of operation (Table 5). Among these 9 failures, only a few failures (3/9) occurred on dams built within the 20th century (highlighted in grey in Table 5). At least 6 failures (6/9) occurred in homogeneous embankments without filters.

Table 5. Failures of large dams after 1900 and after more than 10 years of operation (Foster et al. 1998)

<i>Name</i>	<i>Zoning</i>	<i>H (m)</i>	<i>Completion</i>	<i>Failure</i>
Kantalai	homogeneous	27	612	1986
Emery	homogeneous	16	1850	1966
Utica	homogeneous	21	1873	1902
Avalon II	homogeneous	18	1894	1904
Toreson	?	15	1898	1953
Mill Creek	?	20	1899	1957
Smartt Syndicate	homogeneous	28	1912	1961
Pampulha	Zoned fill	18	1941	1954
Caulk Lake	homogeneous	20	1950	1973

2.5 Failures of large dams initiated in foundations

2.5.1 Failures by Year of construction

The main defects in dam foundations, inherent in the site geology, result in two different failure paths, as follows:

- cracks, where the walls are eroded by the water leaking through them (marked F in Table 6),

- openings, triggering backward erosion or contact erosion of the embankment material through the foundation (marked F+E in Table 6).

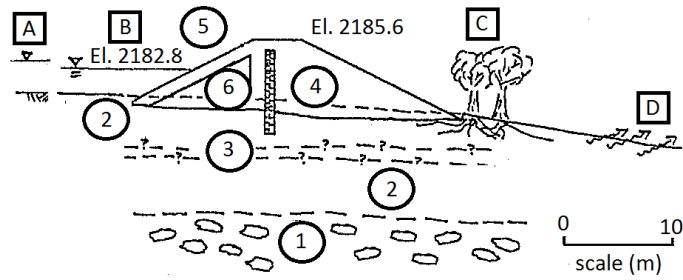
Table 6. List of large dams failures within the 20th century triggered by foundation defects (Foster et al, 1998). The TE type is earthfill and ER is Rockfill.

Name	Type	Construction	Failure	Path
Hauser Lake I	Steel	1906	1908	F
Black Rock (A)	TE/ER	1907	1909	F
Julesberg (B)	TE	1905	1911	F
Horse Creek	TE	1912	1914	F+E
Lake Toxaway	TE	1902	1916	F
Blyderivier	TE	1924	1922	F
Log Falls	TIM	1921	1923	F
Corpus Christi	TE	1930	1930	F
Lower Khajuri	TE/PG	1949	1949	F
Alamo Arroyo Site 2	TE	1960	1960	F
Jennings Creek N°3	TE	1962	1963	F
Baldwin Hills	TE	1951	1963	F
Jennings Creek N°16	TE	1960	1964	F
Nanak Sagar	TE	1962	1967	F
La Laguna	TE	1912	1969	F
Manivali	TE	1975	1976	F+E
Teton	TE/ER	1976	1976	F+E
El Salto	TE		1976	F
Wadi Qattarah	TE	1972	1977	F+E
Ruahihhi Canal	TE	1981	1981	F
Embalse Aromos	TE	1979	1984	F
Quail Creek	TE	1984	1988	F+E
Zoeknog	TE	1993	1993	F+E

2.5.2 Failures initiated in the foundation after more than 10 years: case history of La Laguna dam

The dams highlighted in grey in Table 6 were built during the 20th century and failed after more than ten years. No information was found on Lake Toxaway, and Baldwin Hills was discussed above. La Laguna dam is the only case of failure at long term: it failed after more than 60 years of operation. The embankment comprises an upstream zone of silts and clays compacted by hand and a downstream zone of soil and stones placed in layers. A one meter thick core wall of concrete or masonry separates the upstream and downstream zones. The core wall penetrates 2-5m into the underlying foundation soils. The dam is founded on residual soils (laterite) derived from weathered tuff and basalt. The foundation soils comprise high plasticity silts and clays. Sedimentation tests indicated that the soils did not flocculate in reservoir water (i.e., they were dispersive). Horizontal permeability tests conducted in boreholes indicated that the foundation soils were highly pervious, with permeability in the order of 10⁻⁴ m/s. 'Basaltic pudding', interpreted as weathered basalt with core

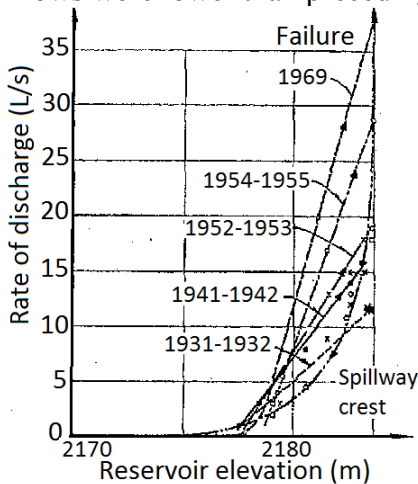
stones, underlies the residual soils. The permeability of this material is also relatively high. Seepage was observed emerging at several locations 10 to 20 m downstream of the dam toe after first filling of the reservoir in 1908 (Fig. 2).



- Legend
- A Spillway crest level
 - B Water level at failure
 - C Large trees
 - D Seepage emerges
 - 1 "Basaltic pudding" weathered basalt with corestones
 - 2 Decomposed tuff and basaltic clays and silts $k=10-4m/s$
 - 3 Volcanic ash layer (depth unknown since first filling - long term increase in flow)
 - 4 Soil and stones
 - 5 Clay
 - 6 wall

Figure 2. The Laguna Dam – section at location of failure.

Seepage flows are measured by two weirs, one on each abutment. The seepage flows on the right abutment are relatively constant with time; however there is an apparent long-term trend of increasing seepage at maximum reservoir level on the left abutment. This is reflected in the plot of seepage vs. reservoir level. Fig. 3 shows the history of seepage measurements for the left abutment from 1927 up to the time of failure. From 1960 to 1968, the reservoir did not reach max reservoir level and the seepage flows were lower than preceding 5 years.



In mid September 1969, the measured seepage flow on the left abutment exceeded the highest previous recorded flow of 30 L/s. This did not cause alarm as the total seepage was 50 L/s lower than the total seepage of 78 L/s recorded in 1942.

Figure 3. Monitoring of leakage at Laguna Dam. Rate of discharge versus reservoir elevation at different years.

During the remainder of September 1969, the reservoir level and all of October remained constant at about Elevation 2182.8, however the seepage flow on the left abutment continued to increase and by October 25 it was 55 L/s. Early in the morning of 31 October 1969, the measured seepage on the left abutment increased again and was 75 L/s. At about

6pm of the same day, a hole with water issuing under pressure was observed on the left abutment. The concentrated leak increased rapidly and started to erode the downstream slope of the dam. At 10:45pm, the masonry cutoff wall was exposed and a few minutes later the embankment was breached.

Photographs taken after the failure show the presence of small piping holes within the weathered volcanic tuff exposed by the breach (Marsal and Pohlenz, 1972). Foster et al. (1998) believe the presence of large trees immediately at the downstream toe of the embankment and tree roots in the foundation may have contributed to the formation of the initial concentrated seepage path. In any case, the internal erosion process was very slow and could have been detected by monitoring.

2.5.3 Failures versus Geology type

Foster et al. (1998) considered it appropriate to use the distribution of geology types from six countries (Australia, Canada, India, New Zealand, UK and USA) to compare the distribution of geology types to world-wide examples of failures caused by internal erosion. The comparison is presented in Table 7 for the both of the principal types of geology: soil and rock. The estimated distributions of foundation geology types for the selected countries are summarized in the right-hand column of soil and rock geology. The estimated distributions of geology types in the failure cases world-wide during the 20th century are summarized in the left-hand columns of both types of geology. Geology types highlighted in grey are over-represented and more susceptible to internal erosion. There is the same number of failures for soil type geology and rock type geology: 10.

Table 7. Comparison of estimated distributions of geology types in the failures to those in dam projects.

SOIL type: 10 failures		ROCK type : 10 failures	
% failures	% of soil type	% failures	% of rock type
50% alluvial	56% alluvial	20% sanstone	21% sanstone
10% glacial	19% glacial	20% shale	21% shale
30% residual	8% residual	40% limestone	7% limestone
	7% colluvial		7% granite
	6% eolian		7% gneiss
	2% marine		7% schist
	1% lacustrine		6% siltite
10% volcanic	1% volcanic	20% volcanic	10% volcanic
			14% others,
100%	100%	100%	100%

The most dangerous situations are:

1. In soil type geology: residual soils and volcanic soils.
 - o The susceptibility of residual soils is associated with dispersive soils (2/3 cases).

- o The weakness of volcanic soils is associated with high permeabilities and voids.
 - o The good performance of glacial soils is associated with slow suffusion processes.
2. In rock type geology: limestone and volcanic rocks.
- o The susceptibility of limestone rock is associated with large cavities.
 - o The weakness of volcanic rocks is associated with large permeabilities and open joins.
 - o The good performance of granite soils is associated with slow suffusion processes. Suffusion is frequent and explains the high number of incidents but suffusion is usually slow enough to intervene before failure.

2.6 Failures of old navigation canal embankments

The Erinoh database contains 45 cases of problems on dikes for navigation or hydropower canals. The retaining embankments of navigation canals, built in France during the 19th century with small widths, no zoning, steep slopes, poorly maintained with little surveillance suffered 14 failures. The locations where internal erosion initiated and the types of situation leading to failures are described in Table 8.

Table 8. The 14 failures of old canal sites (Erinoh)

Canal site	Along adjoining structure	Water tightness protection Contact	Initiation at crest	Uncommon situation?
Arroux	Yes (junction)		Yes	
Montambert	Yes (junction)			Just after long empty period
Houillères		Yes		
Marseille les Aubigny		Yes	Yes	
Micaudière	Yes (aqueduct)			During aqueduct works
Bief partage Vosges	Yes (aqueduct)			
Ponthion		Yes	Yes	
Velaines		Yes	Yes	
Moeuvres				Frost
Languevoisin	Yes			
Allenjoie	Yes?			
Jonchet	Yes (conduit)		Yes	
Briennon		Yes		Fallen Tree?
Masnière		Yes	Yes	

The main causes of failures of these old retaining navigation canal embankments are:

- 1-Internal erosion initiated at junction or transition, in the great majority of these case studies:
 - 1.1 At a contact between soil and structure, or
 - 1.2 Between two watertight materials, or
 - 1.3 Between the watertightness and protection materials.
 - 2-Slopes were stiff: H/V=1,5/1 with protection by concrete slabs or short sheet piles.
 - 3-Desiccation and frost situations were involved in some failures.
 - 4-Leaks were seen several days to several years before failure, in half of these case studies.
- The consequences of failures were low: there were no fatalities.

2.7 Breaches on flood embankments

The ERINOH database completed in 2014, recorded, without being exhaustive, 207 incidents on river embankments in France between the 18th century and today. External erosion (overtopping) caused most of these incidents, but in a large number of old incidents, the cause remains undetermined. Internal erosion has been identified as cause of incidents in 32 % of the total number of cases. In total, 70% of these incidents led to the total breach.

Table 9. Mechanisms leading to incidents on fluvial levees

Mechanism	Total	Internal erosion	External erosion	both erosions	Unknown
Number	207	59	77	6	65
%	100	29	37	3	31

The breaches represent 60% of internal erosion incidents of flood embankments (48 of 65 documented cases); cases of piping erosions without breaching represent 22%. The presence of animal burrows, tree roots or conduits passing through the levee is reported in one third of cases (but given the number of insufficiently documented cases, this proportion should be higher). In the recent years, the delta of the Rhône River was subject to major floods in 1993, 1994, 2002 and 2003. During the 1993 and 1994 floods, 16 partial or total breaches were reported, none due to overtopping. Internal erosion was the mechanism involved in those ruptures, 3 concentrated leaks occurred along pipes crossing levees (3/16) and concentrated leaks after burrowing were identified as the cause of other 13 breaches (13/16).

2.8 Conclusions on failures

- (1) All embankments without filters are at risk of failure by internal erosion. The filter is the most effective barrier against internal erosion. However, design of a good filter is not enough; at least another

safety barrier is required: watertightness of the dam body and of the foundation.

(2) The concentrated leak is the most dangerous mechanisms of internal erosion, amongst the four initiating mechanisms.

(3) The most dangerous defects are openings along adjoining structures (walls and apron of spillway and conduits) followed by cracks through cohesive soils or geologically continuous voids in foundations (open faults, open cracks, karsts).

(4) Only three failures of large dams initiated by internal erosion through the dam body occurred on dams built after 1900 and operated at least 10 years. Two of them presented signs of internal erosion during operation, no information was found on the third breached dam. Careful surveillance should be able to capture such signs and intervention should be able to stop internal erosion on the other dams in operation.

(5) Of the two geology types, soil and rock, the most susceptible to internal erosion of the soils are: residual soils and volcanic soils; and of the rock types are: limestone and volcanic rocks.

(6) The old embankments retaining navigation canals and old flood embankments are very susceptible to internal erosion: upgrading with chimney filter and filter around the pipe, associated with careful surveillance of damages caused by animals and vegetation and of the effects of ageing of transitions, are the main requirements to prevent failure in the long term.

3 LESSONS FROM PHYSICAL MODELS

3.1 The issues

3.1.1 What is the failure process of river dikes constructed of alluvial soils?

No failures of dikes for hydropower canals constructed with alluvial soils have been recorded in the Erinoh database. The design of hydropower canals dikes, built after 1930, mainly after 1950, with zoned embankments, large crest widths, gentle slopes, well-maintained with thorough surveillance, may explain that no failures of modern canal embankments occurred in France. Of the 25 accidents (incidents which did not lead to failure), sinkholes occurred at 9, piping was detected early and stopped at 13, and there were 7 cases of landslides and slope erosions. Most of accidents were triggered by contact erosion or suffusion. The questions are: “how contact erosion and suffusion could lead to breaching of such dikes? Why contact erosion and suffusion triggered less failures than concentrated leaks and backward erosion” (see Table 2).

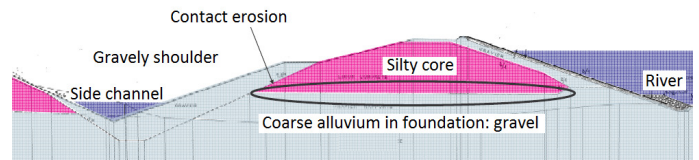


Figure 4: Incident on a river dike caused by contact erosion between core silt and foundation gravel.

Fig.4 shows a dike case study where a typical accident occurred. The contact between the silty core and the gravelly foundation was tested in a physical model in order to answer the question. Usually contact erosion tests are carried out on small scale models 40 to 60 cm long. Sellmeijer (2011) noticed a scale effect in backward erosion. Is there in contact erosion as well? May we rely on the results of the small scale laboratory tests? To answer these questions, a model at 1/1 scale was built and results at small and large scales were compared. The progress of contact erosion was checked by measuring discharge flow, turbidity, settlement and pore pressure.

3.1.2 What is the mode of failure of a zoned dam with filters?

Filters protect dams from internal erosion. However, the filter is a necessary but not sufficient barrier against dam failure caused by internal erosion (see section 2.5). In some situations, the filter can be bypassed by concentrated leaks. For instance, the large silty core of Teton dam was protected by large transition zones. It is the only failure of all the dams designed by the Bureau of Reclamation. More than one hundred large dams were designed successfully by the Bureau with large transitions; so why did this one fail, as shown in Figure 5?

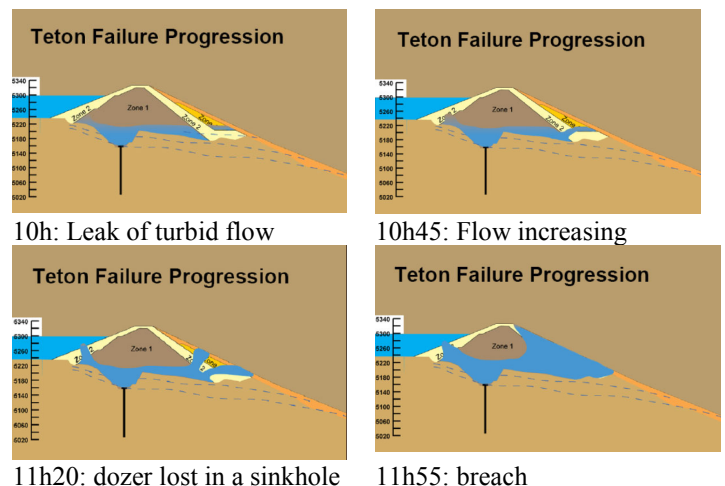


Figure 5: Progression of failure at Teton dam from Snorteland.

The two review panels concluded that piping or seepage erosion was the failure mechanism. The core-to-shell downstream transition zone gradation did not meet either the Bureau of Reclamation criteria or the older, widely accepted Terzaghi-Bertram criteria. Was the gradation the initiator of the fail-

ure? It was only part of the cause of the failure. The failure investigations found open foundation cracks. Most experts who have reviewed the failure agree that there was also hydraulic fracturing of the silty core. Following Sherard's (1987) assumption that the whole base of the core was being eroded in such a manner that the reservoir head was applied at the contact or below the downstream filter, what conditions were necessary for the seepage flow passing along and through the transition filter to crack it and open a hole in the downstream shoulder? Assuming that the safety barrier made by water tightness was broken and the filter was the only safety barrier, what was the other safety barrier, which could have saved the downstream shell from the failure?

3.2 Testing procedure and materials

All tests were carried out at CACOH laboratory (CNR Lyon) in a view of evaluating where and when contact erosion could cause the failure of the levee (Beguin 2011). They were built in a reinforced concrete structure open on its downstream side and upper surface, providing a useful volume 4 m in width, 8 m in length and 2.25 m in height (Fig. 6). The upstream water level was regulated from a reservoir located behind the wall at the upstream end of the test rig. The foundation layer was connected to the reservoir at its upstream and discharged downstream into a settling tank equipped with a spillway. The level of water in the upstream reservoir was increased by successive steps, varying the horizontal flow velocity at the base of the levee. These tests were reported by Beguin (2011).



Figure 6. Construction of the reinforced concrete structure for testing the large scale models.

The tested materials in the foundation are two coarse and pervious rounded alluvium gravels with

narrow grain size distributions: 12/20 mm with $C_u = 1.4$ and 20/40 mm with $C_u = 1.5$ (Figure 7).

The core of the embankment is made of a fine alluvium, a sandy-silt dredged from Bourg-Lès-Valence, one of the most erodible silts of the Rhone, with $d_{50} = 0.14$ mm, $d_{85} = 0.025$ mm and $2\% < 0.002$ mm, $C_u = 85$. The gradings are shown in Fig.7.

The shoulder on the core material is made of:

- Chavanay alluvium: a highly suffusive alluvium $C_u=48$, $27\% < 0.080$ mm; $k=0.001-0.002$ m/s.
- 4/50mm: a stable and very pervious rounded gravel $d_{10} = 5$ mm, $d_{50} = 18$ mm, $C_u = 4$ and $0 < 80$ microns $< 2\%$; $k=0.1$ to 0.18 m/s.

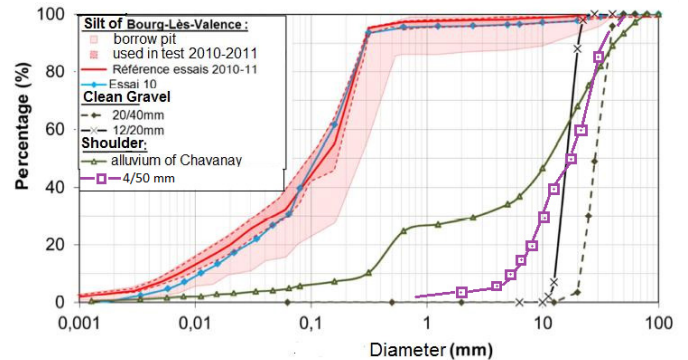


Figure 7. Grain size distribution curves of the core silt, foundation gravels (10/20 & 20/40) and shoulder fill materials : unstable alluvium from Chavanay and stable 4/50.

3.3 First series of models: sinkhole process

The models are focused on the progression of contact erosion at the interface between the gravelly foundation and the silty core of river flood embankments (Fig. 8), compacted in 20 cm thick layers, at a dry density of 1520 kg/m^3 or 92% of standard Proctor optimum density. The foundation material is made of the 12/20 mm gravel. That gravel was too coarse to filter and retain the silt core, and continuing erosion could therefore occur. These two materials were selected in a view to modeling the worst situation of contact erosion.

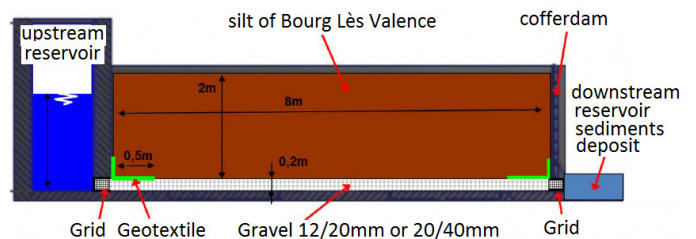


Figure 8. Model for the 3 tests (1, 2 & 3) focused on sinkholes.

Duration of the first test was 99 hours. Four steps of hydraulic load were applied by varying the water level in the upstream reservoir (Fig. 9). During the three first steps, a peak of turbidity and transported fines were observed in water as soon as the step

commenced. The phase of fines transport lasted about one hour and then stopped.

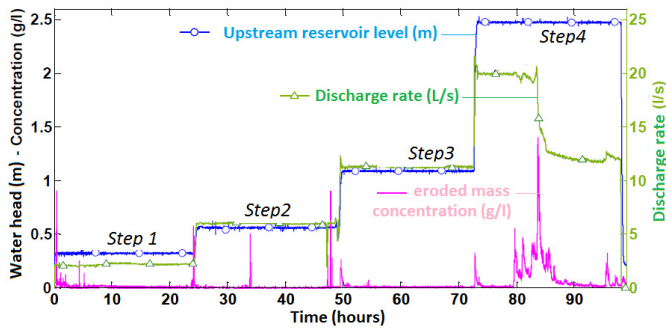


Figure 9. The change of upstream head, discharge flow and turbidity versus time

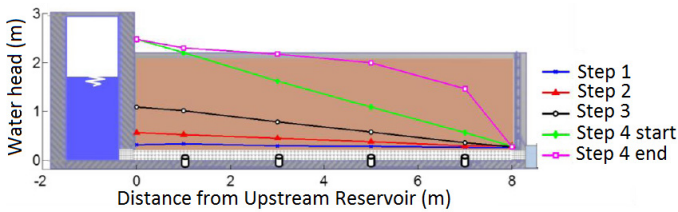


Figure 10. The changes of piezometric line in the gravelly foundation, caused by clogging of downstream toe.

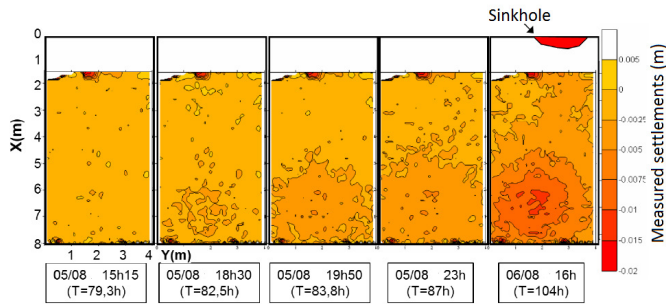


Figure 11. The settlement isocontours in plan versus time.

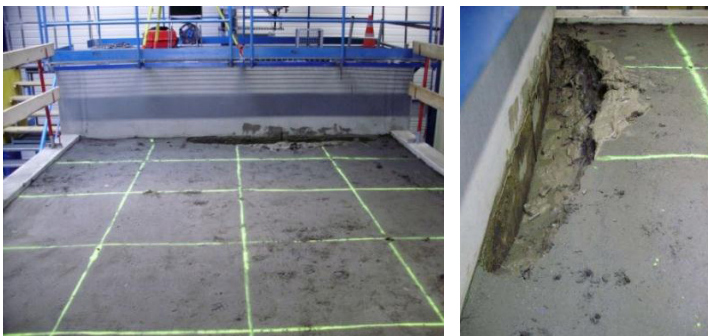


Figure 12. The sinkhole at the end of the test 1 (after 99h).

At Hour 79 during the last step (at an upstream head of 2.5 m and flow rate of 20 L/s), a massive surge of transported fines transport was suddenly triggered. The eroded fines came from the upstream part of the model. At Hour 83, the flow rate began to decrease at constant head. There was a sharp decrease of hydraulic head under the downstream part of the model. This was the consequence of a decrease of the downstream permeability (as shown in Fig. 10). At Hour 84, downstream settlement occurred (Fig. 11). At Hour 96, a sinkhole occurred

along the upstream wall (Fig. 12). At Hour 99, at the end of the test, the flow rate stabilized at 12 L/s, and the turbidity dropped towards zero.

The interpretation of the data is that during the three first steps, erosion at the contact interface was brief, the gravel was merely washed. The massive erosion occurred at the last step under a Darcy flow velocity of 3.5 cm/s and hydraulic gradient of 0.28 in the gravelly foundation. This massive transport of eroded silt leads to clogging of the gravel and a decrease in the flow velocity. This arrested the contact erosion. The sinkhole was observed at Hour 17 following the start of the massive erosion. Its location near the wall was a boundary effect, although it should have been prevented by the geotextile protection! The same process was observed in Tests 2 and 3, but at higher flow velocities and increased erosion rates, with the 20/40 mm gravel in foundation. Interestingly, with the 20/40 mm gravel, the contact erosion was increased and the silt was subject to suffusion: some fine particles were washed out in the sinkhole collapse chimney and sand lenses were founded blocked by the coarsest particles of the silt at the base of sinkhole chimney just above the gravelly foundation (Fig. 13). The coarse particles played the role of a natural filter, stopping contact erosion at their location. However, the contact erosion moved downstream and could cause a second sinkhole (see test 3 Fig. 13).

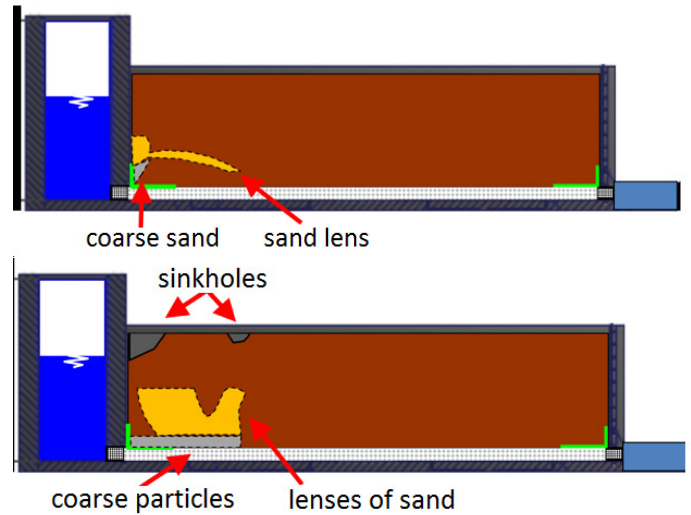


Figure 13. The segregated areas (coarse particles and sand lenses) at the end of the test 2 (above) and 3 (below).

That paving of coarse particles has been observed by Beguin (2011), it decreases the erosion rate and sometimes it stops the contact erosion. This formation of natural filter in alluvium is a first explanation for the low rate of contact erosion and lack of failure in embankment made of fine alluvium on coarse alluvium foundation.

3.4 Second series of models: from contact erosion to concentrated leak erosion

The second series of 8 models (4 to 12) is focused on the progression of contact erosion at the downstream toe of river flood embankments as shown in Figure 14. The fill in the body of the levee was the fine silty alluvium, used in the first series of tests with in addition a thin layer of gravelly fill above the silty shoulder (Fig. 15). The levee was founded on the coarse and pervious rounded alluvium used in the first series (see gradings Fig. 8).



Figure 14. The dike studied in the second series of models (from Beguin 2011).

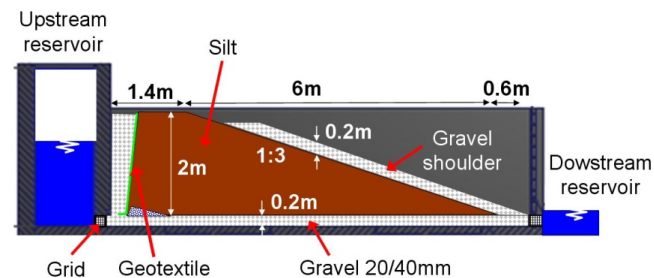


Figure 15. Large scale of levee suffering contact erosion studied in the second series of models (from Beguin 2011).

It is well-known that a granular soil cannot hold a roof (Fell & Fry 2007). Consequently, in a zoned levee, transitions or gravel shoulders should stop piping through a core. Unfortunately, this is not always true. Hydraulic fracture, heave or sliding can jeopardize the filter role. For instance, in tests carried out at CACOH laboratory, CNR and EDF observed that piping could fracture a 20 cm gravelly shoulder of a 2 m high levee prototype.

As the Darcy flow velocity passed 2 cm/s in the gravel, the turbidity at the downstream toe increased. The flow began to carry away the gravel from the downstream shoulder. After a period of time lasting from several minutes to several hours, a true erosion pipe emerged on the downstream face and through it

a very substantial flow was discharged as shown in Figure 16.



Fig.16: Piping exit in a levee suffering contact erosion (from Beguin, 2011).

Based on this result, it appears that contact erosion could lead to the failure of levees if the following four conditions are met.

- (1) There is continuing erosion between gravel and silt (i.e. no filtering, when $9.d_{85\text{core}} < d_{15\text{shoulder}}$);
- (2) The Darcy velocity is higher than 2 cm/s in the gravel;
- (3) The pipe in the core does not collapse.
- (4) The shoulder fill layer is too thin.

As no failures of EDF or CNR levees have been caused by contact erosion during the last 60 years, at least one of the four conditions did not occur on site. In reality, the downstream shoulder is thicker than that modeled. This leads to the next question: “could the piping be stopped by a thicker gravelly shoulder?”

To answer that, another large scale test was carried out with a 130 cm (vertical) deep gravel shoulder. The shoulder material was also changed, to be more representative of the suffusive used alluvium (Fig. 8) or in the terminology used by Kenney & Lau (1985, 1986), susceptible to internal instability.

Although the upstream head was 2.1 m and contact erosion of the silt was continuing at a Darcy flow velocity higher than 2 cm/s in the foundation, no failure occurred after several days of continuing erosion. The test was repeated twice to be sure that the 1.3m thick shoulder could withstand the hydraulic forces imposed on the shoulder fill by the water head emerging from the foundation (Table 9).

Table 9. Results of contact erosion tests with 1.3m thick shoulder.

Test	Initiation		Progression Eroded silt mass (kg)	Failure	Visual in- spection
	V (cm/s)	i			
2.1	2.6	0.23	965	no	Sinkhole in progress un- der the crest
2.2	2.9	0.23	1625	no	Leakage with unraveling, but which soon stopped
2.3	2.3	0.15	675	no	-

In Test 2.2 global backward erosion occurred and excavated a gully from the toe to the top of the slope as shown in Figure 17. It looked similar to the upward erosion observed on the downstream face of the Teton dam.



At 10h53'10'' after 50h02 of test



At 10h53'13''



At 10h53'15''



At 10h54'57''



At 10h56'00''



At 11h10



At 11h51' after 53,7h of test



End of test 10/08/2012 at 8h after

Figure 17: Progression of erosion on the downstream face of test 2.2

The reason for this upward progression is the clogging of the shoulder by eroded silt. The materials appeared to be less compacted and the silt dryer in

Test 2.2 than in the other tests. The exit of the flow was plugged by the eroded silt, and the erosion of the shoulder fill progressed upwards near the surface of the slope (Fig. 18).

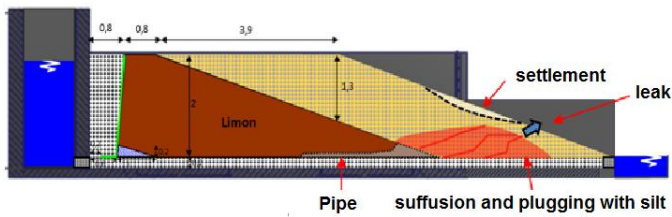


Figure 18: Interpretation of the progression of erosion on the downstream face of test 2.2

These former tests have demonstrated that a thick shoulder can stop piping through the core, the latter that a thin shoulder cannot: what is the minimum thickness of the downstream shoulder to prevent the failure of the levee?

3.5 Third series of models: global backward erosion

3.5.1 Objective and testing procedure

In this third series, only the behavior of the shoulder fill was studied. to resolve the previous question by determining both the mechanism of shoulder failure and the criterion for protecting the shoulder from the failure. Three different mechanisms of failures may occur: (1) general instability without hydraulic fracturing, (2) hydraulic fracturing followed by piping, (3) backward erosion and surface plane sliding.

Two kinds of materials were used in the shoulder: the pervious and stable 4/50 and the suffusive alluvium of Chavanay (Fig. 8).

3.5.2 Shoulder with pervious and stable gravel

Two kinds of flow were injected at the base of the shoulder:

- 2D with 5 injector pipes (see Plan View Fig. 19)
- Concentrated leak by a single central pipe.

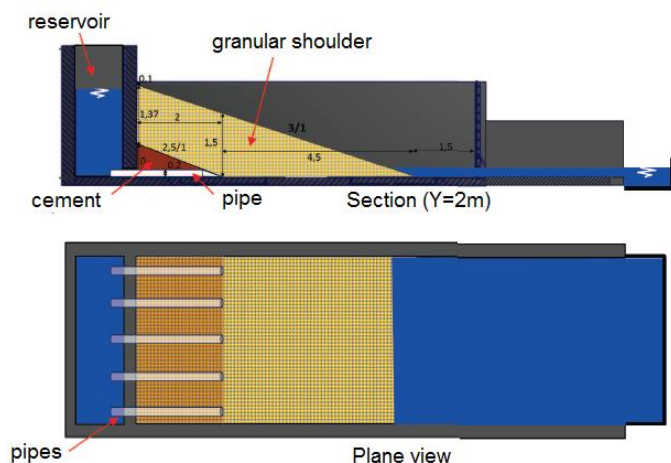


Figure 19. Sketch of the third series of models (Beguin 2011).



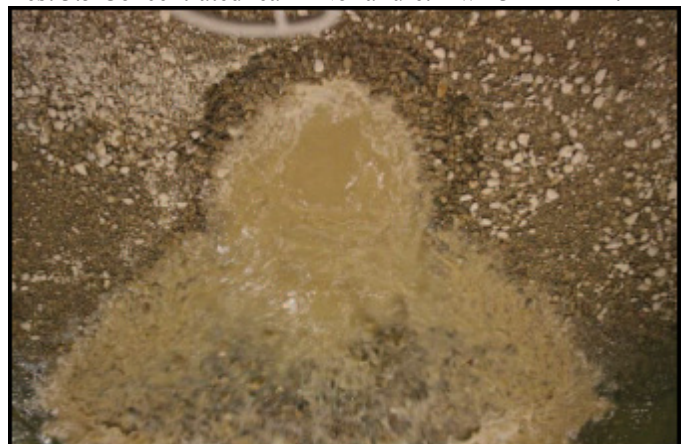
Test 3.1 2D flow erosion initiation $H_w=0.9$ m shoulder thickness $h=1.5$ m



Test 3.1 2D flow - Failure. $H_w=1.66$ m $h=1.5$ m.



Test 3.5 Concentrated leak - No failure. $H_w > 3$ m $h=1$ m.



Test 3.7 Concentrated leak $H_w > 3$ m $h=0.5$ m. Heave & backward erosion on a stable gravel.

Figure 20. Progression of erosion or not with a very pervious shoulder.

The very pervious material was lightly compacted by 2 passes of vibrating plate ($\rho_d = 1760 \text{ kg/m}^3$ and $w = 2\%$).

The shoulder fill could withstand the very high water heads imposed by the concentrated leak emerging from the erosion pipe (see test 3.5 in Table 10). Very high head loss was measured in the shoulder near the pipe exit in test 3.5, resulting in the lack of failure even with 1 m thick shoulder resisting 3.05 m reservoir head (see test 3.5 in Figure 20). Hydraulic heave did not occur with 3m reservoir head.

The reservoir head causing failure is much lower, where the flow is 2D (see test 3.1 in Table 10). The results are compiled in Table 10.

Table 10: Results of very pervious shoulder tests.

Test	Shoulder thickness	Type of flow	Reservoir head at failure	Visual inspection of the mechanism
3.1	1.5 m	2D	1.66 m	Global Backward erosion. Progressive heave
3.5	1.5 m reduced to 1 m	Concentrated leak	> 3.05 m	No failure
3.7	0.5 m	Concentrated leak	3.05 m	Backward erosion and sudden blow-out

3.5.3 Shoulder with suffusive alluvium

The suffusive alluvium was tested because it was at first sight the worst type of shoulder fill due to the potential for suffusion. The average gradation of the alluvium is shown on Figure 8. The initial state was $\rho_d = 2100 \text{ kg/m}^3$ and $w = 4\%$. The mechanism of failure it was markedly different to that through the very pervious shoulder, it developed in the following phases.



Dike crest (plan view)

(1) Surface sliding caused by 2D flow under the shoulder made of suffusive alluvium.

Toe



Crest

(2) Horizontal crack and sudden increase of discharge flow through the crack.



Toe
Crest

Leak

(3) Scour or sloughing downstream and below the crack.

Downstream toe

Figure 21. Photos of the failure of a shoulder made with alluvium caused by 2D flow.



(1) local sliding and crack caused by the concentrated leak under the shoulder made of suffusive alluvium.



(2) Horizontal crack and sudden increase of discharge flow through the crack.



(3) Scour or sloughing downstream and below the crack.

Figure 22. Failure of a shoulder made with suffusive alluvium caused by a concentrated leak.

3.6 Interpretation

3.6.1 Scale effect in contact erosion

The comparisons between the critical hydraulic gradients in Fig. 23 and the Darcy flow velocities in Fig. 24 respectively, measured in small scale apparatus and those measured in the large scale apparatus shows the influence of the thickness of the gravel layer.

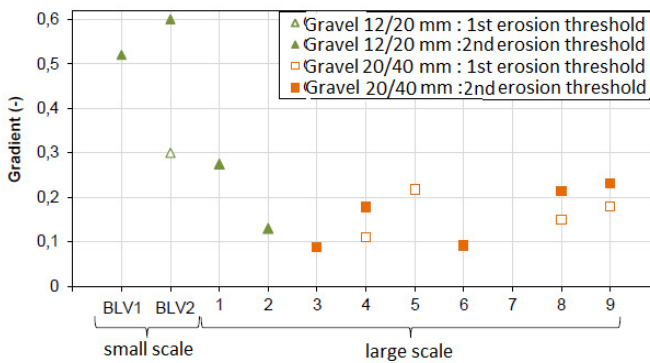


Figure 23. Critical hydraulic gradients at small and large scales.

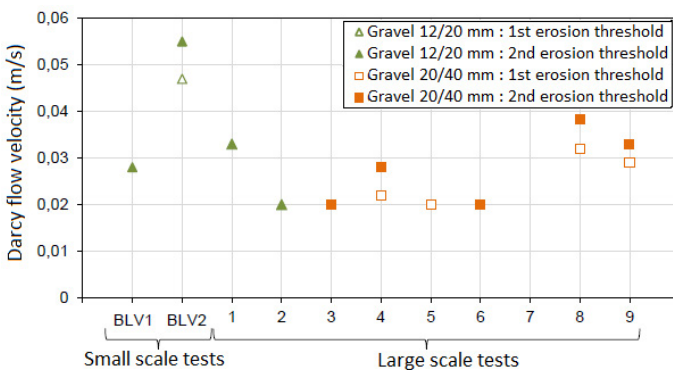


Figure 24. Critical hydraulic Darcy flow velocities at small and large scale.

Higher critical hydraulic gradients occurred when the gravel layer was clogged by the transported fines. Thinner is the gravel layer, larger is the clogging and larger are the threshold values: that is the explanation of the higher values at small scale. The scatter of the critical values of the hydraulic gradient is larger than the scatter of the critical values of the

Darcy flow velocity. The minimum critical value of Darcy flow velocities at small scale, 2 cm/s, is equal to the minimum value of Darcy flow velocities at large scale (It is not the same for the hydraulic gradient). According to the large pore sizes of the gravel, the permeability is not constant: it follows the Forcheimer relationship; the Darcy flow velocity gives a better threshold of contact erosion. Based on that result, we can conclude that with enough thick gravel layers, there is no scale effect on the critical value of Darcy flow velocity. However the critical hydraulic flow velocity can be increased by clogging of the thin gravel layer (< 20 cm).

The observed critical flow velocity is the start of a continuing transport of fines, eroded from the silt contact. It does mean than below that critical flow velocity there is no erosion. The figure 25 shows the trend of the erosion rate measured in the first 30 minutes of the tests: the threshold value is not seen on that figure.

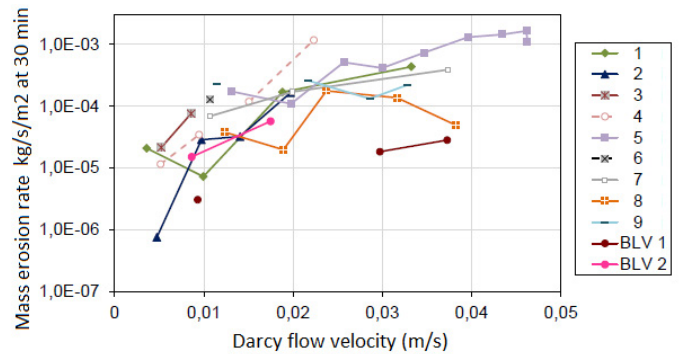


Figure 25. Mass erosion rate versus measured in the 2 small scale tests and the 9 large scale tests (Beguín 2011).

Erosion occurs with a Darcy flow velocity lower than the critical value, however that erosion decreases and stops quickly; after the transport of the finest particles, the largest particles lay down on the contact and do a temporary open filter, up to a new increase of the flow velocity.

The laboratory tests capture only short term phenomena. The influence of little changes of hydraulic heads occurring during small floods on long term is not simulated in the laboratory. This effect does not look negligible. On some river embankment, linear settlements versus time are observed. The estimated settlement rate is between 2mm/year and 1cm/year. The mass erosion rates associated with the previous settlement rates in the foundation are between 1E-10kg/s/m² and 5E-10kg/s/m², far below the measured erosion rate in laboratory. This erosion is supposed to be triggered by Darcy flow velocity below the critical value.

3.6.2 Effect of suffusion

It is interesting to note that the effect of suffusion on the behavior of the unstable Chavanay gravel has three phases: the first is the detachment and

transport of fines, the second is the clogging of gravel by transported fines leading to a decrease of permeability (Fig. 26) and the third is the hydraulic fracture leading to crack formation and sudden release of leakage. The initiation of the first step was difficult to observe, the second step was observed under a large range of values of hydraulic gradient and the third step triggered the shoulder failure or backward erosion. It is difficult to define a critical value of the hydraulic gradient from the measurements of permeability in the oedo-permeameter of the GeM (Fig.26).

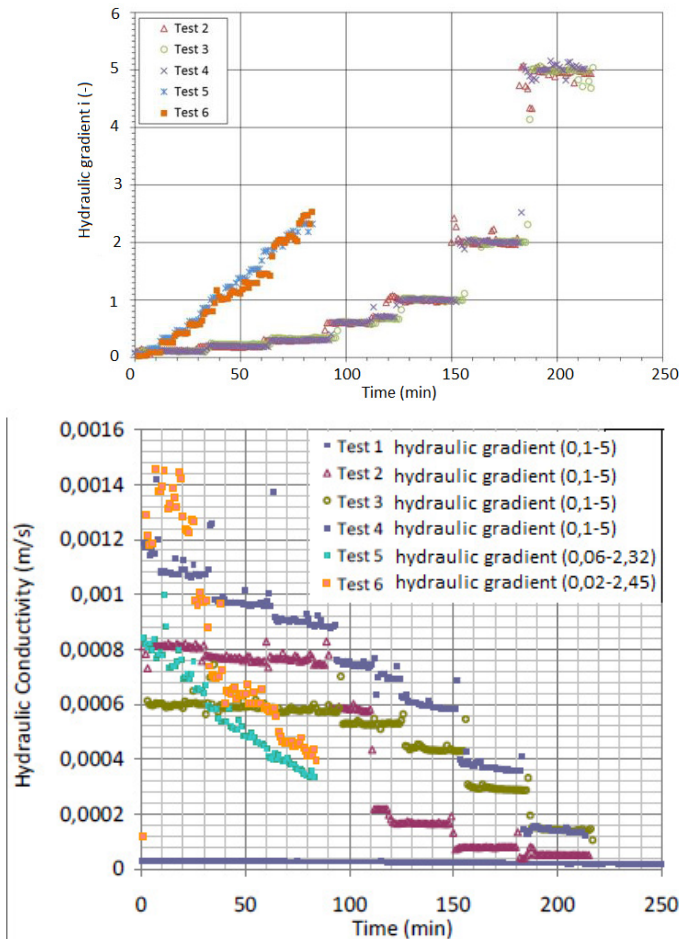


Figure 26. Hydraulic gradient and permeability of the Chavanay gravel (Marot & al 2014).

In some experiments the permeability has been decreasing since the lowest value of the hydraulic gradient, in some others there is a clear decrease for hydraulic gradients i higher than 0,6. The value $i_c=0,6$ is in agreement with the critical hydraulic gradient defined by Li (2008). However the scatter of the critical hydraulic gradient is one more time observed in the large scale tests. In Figure 27, the critical gradient $i_c=0,6$ is compared to the calculated hydraulic gradient nearby the pore pressure cell detecting in the large scale tests a first change and a large change of pore pressure, assuming signs of massive transport of fines. From the pore pressure cells the critical hydraulic gradient increase with the vertical stress (the height of the shoulder). This point needs clarification.

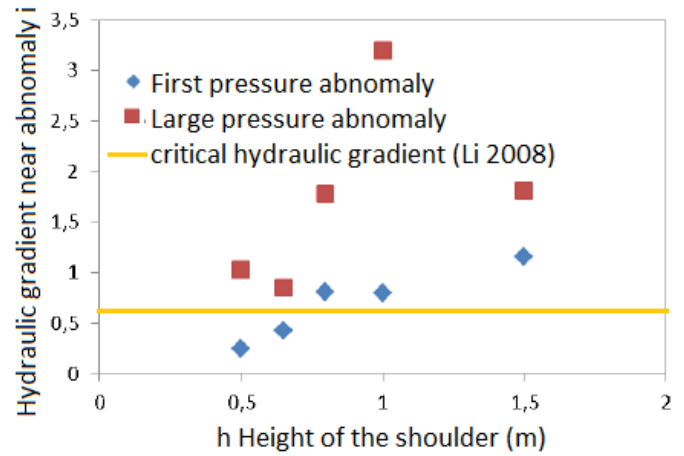


Figure 27. Comparison of critical hydraulic gradients for the suffusive Chavanay alluvium.

3.6.3 Hydraulic fracturing and instability

Hydraulic fracturing may have occurred causing first the crack and secondly the leak in the large scale tests and contributed to the local or global sliding. The hydrostatic pore pressure in the reservoir at failure was equivalent to the total normal stress on a plane parallel to the downstream face (equation 1) for 2D flow, and higher for a concentrated leak. Thus, the effective normal stress $\sigma'_n = 0$, applied at the exit of the pipe, should be a criterion for the failure of the semi-pervious downstream shoulder subjected to the pressure of 2D flow, and a conservative one for shoulder protecting the dam core from a concentrated leak. The results of comparisons between calculated total stress σ_n and measured pore pressure u at failure are compiled in Table 11.

$$\sigma'_n = \gamma \cdot h \cdot \cos^2(\beta) - u \quad (1)$$

With σ'_n effective normal stress, γ wet unit weight of the shoulder, h thickness of the shoulder (vertical distance), β slope angle and u pore pressure.

Table 11. Results of shoulder tests with suffusive alluvium.

Test	Shoulder thickness (m)	Type of flow	reservoir pressure at failure (kPa)	Total stress (kPa)	Visual inspection of the mechanism
3.2	1.5 m	2D	28	29	Sliding
3.3	1.5 m	2D	29	29.7	Sliding
3.4	0.5 m	Concentrated leak	11,3	9.3	Local sliding, crack and scour
3.6	1 m	Concentrated leak	>30	19	No failure
3.8	0.65 m	Concentrated leak	15,7	12.7	Local sliding, crack and scour

3.6.4 Application and discussion

For assessing the safety of a zoned dam or a zoned levee, focusing on the risk of internal erosion, a distinction has to be made between two shoulder types:

- Shoulders with very large drainage capacity (in these cases discharge flows from concentrated leaks are far lower than the discharge capacity of the shoulder or permeability larger than 0.1 m/s, i.e. rockfill or clean gravel) and,
- Shoulders with fair drainage capacity (discharge flow from concentrated leaks similar to the discharge capacity of the shoulder or permeability around 0.001 m/s, i.e. alluvium).

The large drainage capacity shoulders have to be protected from backward erosion. This phenomenon is sometimes observed when an extreme flood occurs during construction of CFRD (concrete faced rockfill dams), before the concrete slab placing. It was the cause of the failure of Hell Hole dam (1964). It occurred on the 4th February 2014 at Tokwe-Mukorsi dam (Fig. 28).



Figure 28. Backward erosion during the construction of the Mokwe Mukorsi CFRD dam

To protect this type of shoulders from backward erosion, the smallest blocks and more graded curve with low permeability and high density are placed in the dam center and the largest rip-rap blocks are placed on the downstream face. The slope has to be designed using the Kovacs (1981) relationship and the refined Solvik equation (3) by EBL Kompetanze (2003) or the Knauss equation (1975) or Martins relationship (1982).

The three last equations give close dimensioning of the block diameters versus the slope and the unit discharge flows (Fig. 29).

$$D_{50} = 0,6 \cdot S^{0,43} \cdot q^{0,78} \quad (3)$$

With D_{50} the mean diameter of downstream blocks in m S the slope (V/H) and q the unit discharge flow in $m^3/s/m$.

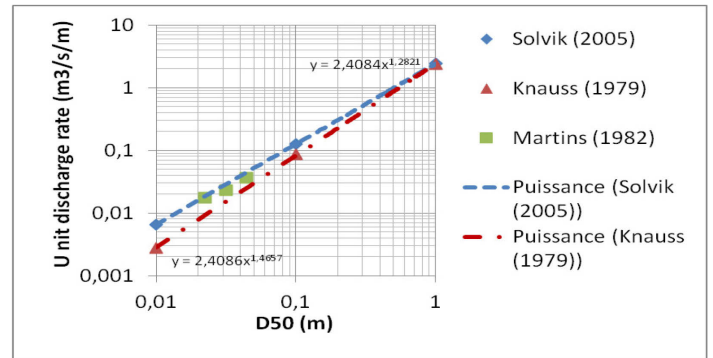


Figure 28. Dimensioning of D_{50} versus unit discharge flow by, Knauss (1979) Martin (1982) and Solvik (2005)

The fair drainage capacity shoulders have to be protected from sliding and hydraulic fracture. The criterion of effective normal stress equals to zero can be used (equation 2). From this point of view, thick cores ($H/V=1/1$) lead to less safe downstream shoulders than thin cores (a larger core implies a thinner shoulder but a similar maximum water head at the end of the pipe).

$$\tan(\beta) \leq \sqrt{\frac{1}{F} \left(\frac{\gamma \cdot h}{\gamma_w \cdot h_w} \right) - 1} \quad (2)$$

For instance, applying this criterion using equation (2), (with the notations given with equation 1 above, and F meaning Factor of Safety) to the downstream toe of the core of Teton dam, shown on Figure 5, concludes that the shoulder cannot withstand the pressure. At Teton with $h_w=36$ m and $h=18$ m, $\gamma/\gamma_w=2$ and $F=1$, $\tan(\beta) < 0,33$ meanings that the D/S slope should be $H/V > 3$ when it was $H/V=2,5$ at elevations higher than 1585 m. Conversely, applying the same criterion to the near failure of Fontenelle concludes that the shoulder could withstand the pressure. However, if the reservoir had not been dropped, backward erosion would have eroded the core. This means that another condition has to be explored: the hydraulic condition and the kinetics of the erosion rate. More work to integrate this condition is needed and will be published in due course.

4 CONCLUSION

Assessment of case histories of dam failures give crucial lessons for practitioners. Embankments without filters are at risk of failure by internal erosion. No failure of large dam with a good filter at the good location is reported. However, design of a good filter is not enough, the watertightness of the dam body and of the foundation is the second safety barrier required. In most of the dams, the failure initiated with concentrated leak passing through defects. And in most of the cases, the defects are openings along adjoining structures and cracks through

cohesive soils or geologically continuous voids in foundations (open faults, open cracks, karsts). Only three failures of large dams initiated by internal erosion through the dam body occurred on dams built after 1900 and operated at least 10 years. Two of them presented signs of internal erosion during operation, no information was found on the third breached dam. Careful surveillance should be able to capture such signs and intervention should be able to stop internal erosion on the other dams in operation. The most susceptible soils to internal erosion are residual soils and volcanic soils. The most susceptible rocks are limestone and volcanic rocks.

Large scale physical models give other lessons on contact erosion, suffusion and backward erosion. No scale effect was noticed on the critical Darcy flow velocity. However fines transport can plug thin gravel layer and increase the critical value of the hydraulic gradient. Darcy flow velocity in gravel higher than the critical value could lead to concentrated leak at the base of the core. Thanks to thick alluvium shoulders, the concentrated leak could not lead to failure by piping. There is a critical value of the height of the shoulder on large silty cores with semi pervious or unstable gravel in the shoulders for preventing the zoned dams or levees from the hydraulic fracture and failure. For very pervious gravelly shoulder (rockfill) the revised backward erosion criterion of Solvik could be used.

5 REFERENCES

- Beguín, R. 2011. Etude multi-échelle de l'érosion de contact dans les ouvrages hydrauliques. Thèse de l'Université Joseph Fourier Grenoble
- EBL Kompetanse 2003. Stability of downstream shell and dam toe during large through flow, Stability and breaching of embankment dams. SP2. Publikasjons nr: 186-2005.
- Fell, R. & Fry, J.J. 2007. Internal Erosion of Dams and their Foundations. Taylor & Francis ed.
- Foster, M. & Spannagle, M. & Fell, R. 1998. Report on the analysis of embankment dam incidents. UNICIV Report No.R374, School of Civil and Environmental Engineering, University of New South Wales ISBN: 85841 349 3; ISSN 0077-880X.
- Fry, J.J. Beguín, R. Picault, C. Mathieu, F.Esnault Filet, A. Mosser, J.F. 2015. Analyse et traitement de l'érosion interne : procedes classiques et nouveaux. ICOLD Congress Stavanger. Q98.
- Hoffmans (2011) The influence of Turbulence on Soil Erosion Eburon Academic Publishers
- ICOLD, 1994. Embankment Dam. Granular Filters and Drains. Review and Recommendations. Technical Bulletin 95. CIGB-ICOLD, Paris.
- ICOLD, 1995. Dam failures Statistical Analysis. Technical Bulletin 99. CIGB-ICOLD, Paris.
- ICOLD, 2015. Internal Erosion of Existing Dams, Levees and Dikes, and their Foundations. Volume 1: Internal Erosion Processes and Engineering Assessment. Technical Bulletin 164. CIGB-ICOLD, Paris.
- Kenney, T.C. & Lau, D. 1985. Internal stability of granular filters. Canadian Geotech. J., Vol. 22, 215-225.
- Kenney, T.C. & Lau, D. 1986. Closure to: internal stability of granular filters. Canadian Geotech. J., Vol. 23, 420-423.
- Knauss, J. 1979. Computation of maximum discharge at overflow rockfill dams (A comparison of different model test results) ICOLD Congress New Delhi. Q50 R9 pages 143-160.
- Kovacs, G. 1981. "Seepage Hydraulics". Elsevier Scientific Publishing Company, Amsterdam, The Netherlands. 730 p.
- Li, M. 2008. Seepage induced instability in widely graded soils. PhD-thesis. The University of British Columbia. May 2008.
- Marot, D. Bendahmane F. Chuheng Z. 2014. aractérisation de l'érodabilité d'échantillons de sols du Chavanay (0-50mm) Rapport d'essais 18-07-2014 GeM.
- Marsal, R.J. and Pohlenz, W. 1972. The failure of Laguma Dam. Performance of Earth and Earth-Supported Structures, ASCE, Vol. 1, pp. 489-505.
- Martins, R. 1982. Overflow Rockfill Dams. ICOLD Congress Rio de Janeiro. Q55 R23 pages 405-419.
- Richards, K.S. & Reddy, K.R. 2007. Critical appraisal of piping phenomena in earth dams. Bull Eng Geol Environ (2007) 66:381-402. DOI 10.1007/s10064-007-0095-0.
- Sellmeijer, J.B. 1988. "On the mechanism of piping under impervious structures", PhD thesis, Delft University of Technology, The Netherlands, 1988.
- Sherard, J.L 1987. Lessons from the Teton Dam Failure, Engineering Geology, 24, Elsevier Science Publishers, pp.239-256.
- Snorteland, N. 2009. Teton Dam Failure in CEA lessons learned. USBR. Presentation.